Left Ventricular Volume Calculation Using a Count-Based Ratio Method Applied to Multigated Radionuclide Angiography

Teresa Massardo, Rami A. Gal, Raymond P. Grenier, Donald H. Schmidt, and Steven C. Port

University of Wisconsin Medical School, Milwaukee Clinical Campus and Sinai Samaritan Medical Center, Mount Sinai Campus, Milwaukee, Wisconsin

The purpose of this study was to investigate the accuracy of a new count-proportional method for the measurement of left ventricular volume when applied to gated equilibrium blood-pool imaging. An equation is developed that relates total chamber volume, V_t, to the area of a pixel (M) and the ratio (R) of total counts within the chamber to the counts within the hottest pixel in the chamber such that $V_t = 1.38\ M^3R^{3/2}$. The value of M is a constant for the particular scintillation camera-collimator system and R is obtained from observed count rates. All calculated volumes were compared to volumes measured using biplane contrast ventriculography. In 25 patients, the method for ventricular volumes gave an r of 0.95 and an s.e.e. of 23 ml [Volume (nuclear) = 0.94 Volume (cath) + 1.3]. End-systolic volume was best calculated from end-diastolic volume and ejection fraction. Manual regions of interest were more accurate than automated regions of interest. This method appears to be as accurate as more complex approaches and has the advantage of not requiring attenuation correction or blood sampling.

J Nucl Med 1990; 31:450–456

The first non-invasive radionuclide angiographic (RNA) approach to left ventricular volume determination was a geometric technique applying the formulas used in contrast angiography (*1*). Other authors have also utilized geometric techniques (*2–6*). The disadvantages of the geometric methods include the limited resolution of RNA studies and the application of a prolate ellipsoid model to ventricles in which dilatation or wall motion abnormalities distort the shape (a limitation inherent in most geometric approaches). An early nongeometric approach used dilution curve analysis (*7,8*) but was also shown to have significant limitations (*9*). Count-proportional, nongeometric methods are based on the fact that the radioactivity recorded from a chamber, at equilibrium, is proportional to the volume of the chamber. Sorensen et al. showed that stroke counts were directly related to stroke volume measured invasively (*10*) and both Slutsky et al. (*11*) and Dehmer et al. (*12,13*) calculated absolute volume from chamber activity. The latter required peripheral blood sampling to determine the counts/ml of a reference volume and applied a regression equation obtained by comparison to contrast angiographic volumes.

That approach is compromised by the attenuation of left ventricular counts and the lack of attenuation of counts from the reference volume. A method to correct for photon attenuation using the attenuation factor of water (μ:0.15 cm^{-1}) has been proposed by Links (*14*) and also used by others (*15,16*). However, the assumption that the density of the whole chest is similar to that of water has been amply disputed. The range of the attenuation factor has been estimated to be 0.08 to 0.16 cm^{-1} (*11–22*).

Maurer (*23*) reported the use of an intraesophageal source to calculate a transmission factor for individual determination of attenuation. Harpen (*24*) used a transmission factor from a first-pass acquisition. Another approach to solve this problem was the use of a "build-up factor," which also attempted to correct for scatter activity (*25,26*). The methods that correct for attenuation require a measurement of the distance from the center of the left ventricle (LV) to the collimator. That was commonly obtained through a trigonometric function using a static anterior view (*18*) or a two-dimensional echocardiographic technique (*16*). A last approach has used SPECT with a known voxel size and no background correction; however, that is a very complex and time-consuming method (*27*).

Bourguignon (*28*) has developed a method of volume calculation based on aortic arch counts and background correction (that should be similar in the aorta and LV) without blood sampling.

A count density distribution method has also been described (*29–31*) and applied to first-pass RNA acquisitions. That approach was based on a measurement of

Received Oct. 24, 1988; revision accepted Oct. 31, 1989.

For reprints contact: Steven C. Port, MD, Cardiovascular Disease Section, Sinai Samaritan Medical Center, 950 N. 12th St., Milwaukee, WI 53233.

the ratio of total counts to peak pixel counts in the LV. The ratio was shown to be a function of the volume. That technique is particularly attractive since neither attenuation correction nor blood sampling is required. In the present report, we expand on that particular count-based theory and describe its application to multigated equilibrium radionuclide angiography (EqRNA) (*32*).

METHODS

Count Proportional Volume Theory

From a homogeneously mixed volume of a gamma emitting tracer, the total number of gamma rays that pass through a multichannel collimator (total count) is proportional to the volume, independent of its shape. The maximum pixel count is proportional to an effective reference volume defined as the product of the length of the longest axis perpendicular to the collimator and the cross-sectional area of the pixel. The constant of proportionality can be eliminated by forming the ratio of total counts to maximum pixel counts.

That ratio is fundamentally a measure of the number of reference volumes contained in the total volume. The key, then, to the determination of total volume is to determine the exact volume of the reference volume. For many volume shapes (e.g., spheres, ellipsoids, cylinders), the reference volume is readily determined.

In general, a reference volume theorem is defined as follows: the reference volume (cm^3) is always equal to the pixel area (cm^2) times the longest axis (cm). The reference volume theorem can be proven for a broad class of parallel-hole multichannel collimators, including all the collimators used in practice with scintillation camera systems. The theorem is independent of the spatial resolution, the efficiency of the collimator, the shape of the collimator holes, or the distance of the source from the collimator. The rigid and formal mathematical proof of the reference volume theorem is beyond the scope of this article; however, empirical proof of this theorem is easily obtained by measuring a variety of known volume distributions with any gamma scintillation camera at different distances from the collimator, with different collimators and with different sampling matrices.

The practical applications of the reference volume theorem can be simply illustrated by using a spherical volume of distribution as an example. Let a spherical volume of diameter, D, filled with a homogeneous solution of gamma-emitting tracer, be measured with a multichannel collimator/scintillation camera system using a sampling matrix with pixel dimension equal to M, in cm, so that the cross-sectional area of each pixel is equal to M^2. The reference volume theorem states that the reference volume, V_r, is equal to M^2D. In this example, the pixel which samples V_r is clearly the pixel with maximum counts, (N_m). N_m is proportional to V_r, hence:

$$N_m = KV_r = KM^2D, \quad (1)$$

where K is the constant of proportionality with dimensions counts/cm^3. The total counts, C_t, is proportional to the total volume of the sphere, V_t, hence:

$$C_t = KV_t = K/6D^3. \quad (2)$$

The constant of proportionality is eliminated by taking the ratio $R = C_t/N_m$ which from Equations 1 and 2 is as follows:

$$R = \frac{C_t}{N_m} = \frac{KV_t}{KV_{ref}} = \frac{V_t}{V_{ref}} = \frac{/6D^3}{M^2D} = \frac{/6D^2}{M^2}. \quad (3)$$

It is clear that R is a dimensionless quantity that is equal to the number of reference volumes contained in the entire spherical volume.

Equation 3 may be solved for D as follows:

$$D = 6M^2R. \quad (4)$$

The volume of the sphere is:

$V_t = /6D^3$, hence from Equation 4,

$V_t = /6\ 6M^2R^3$

or,

$$V_t = 1.38\ M^3R^{3/2} \quad (5)$$

The volume of the sphere, in cm^3, is directly obtained from Equation 5 since M is known for any pixel matrix and R is the observed count ratio.

Patient Population

Twenty-five patients were prospectively studied, 16 of them males and 9 females, with a mean age of 62.8 and a range of 38 to 83 yr. They were recruited from the population undergoing routine diagnostic catheterization. The only selection criteria were the patient's clinical stability, the possibility of performing a biplane left ventriculogram prior to any other angiography, and the availability of the portable gamma camera. Documented informed consent was obtained from all patients.

Radionuclide Acquisition

EqRNA was performed in the catheterization laboratory immediately after arterial access was obtained and before biplane angiography was done.

In vivo red cell labeling was used with injection of 1.2 mg of Sn-pyrophosphate followed, 20 min later, by 925 Mbq (25 mCi) of technetium-99m-pertechnetate. The best combination of left anterior oblique and caudal angulations was selected for separation of the two ventricles. The RNA was performed with a portable, small field of view (200 mm) gamma camera equipped with an all-purpose, low-energy, parallel-hole collimator. Data were acquired in frame mode using 24 frames per cycle, a matrix of 64×64 pixels, an energy window of 140 keV ± 10% and a beat-rejection window of 15%. Beats within the window were interpolated "on-the-fly" so that a uniform LV time-activity curve was generated. The acquisition was stopped at pixel saturation and total counts averaged 6-8 × 10^6.

Data Processing

The LV ejection fraction (EF) was calculated in the 25 studies using automated and manual programs. With the automated method, the regions of interest (ROI) were generated using a second derivative edge detection threshold. A semicircular shaped background ROI was created around the LV on the end-systolic (ES) frame, and average counts per

pixel in the background ROI were subtracted from the time-activity curve. With the manual approach, the ROI were drawn manually at end-diastole (ED) and end-systole. The same background subtraction method was used. Both the manually-drawn and the computer-generated ROI for ED and ES were recorded and later applied to the original raw data in order to calculate the ED and ES volumes.

The total raw counts in the LV ROI both at ED and ES were determined as well as the maximum pixel count (N_m). In order to minimize statistical errors an average of the four highest pixels was used to calculate N_m.

1. Knowing LV counts and LV N_m at ED and ES, the ratio $R = \frac{\text{Total Counts}}{N_m}$ is calculated.
2. M, or size of the pixels, was 0.344 cm. The formula in Equation 5 for the volume of a sphere, 1.38 $M^3R^{3/2}$ was then applied to both ED and ES.

This method was used with both manual and automated ROI. Although ES volume was calculated directly, as mentioned above, it was also derived by using the EF and the calculated ED volume. For reproducibility, the manually-drawn ROI were performed by a second observer. Both intraobserver and interobserver variation were analyzed for ED and ES volumes.

Contrast Angiography

Left heart catheterization and coronary arteriography were performed using standard techniques. Simultaneous biplane contrast ventriculography was performed in 30-degree right anterior oblique (RAO) and 60-degree left anterior oblique (LAO) views at 30 frames/sec for each view using 30–50 ml of diatrizoate meglumine. Left ventricular volumes and EFs were calculated using the biplane approach of Dodge and Sandler (*33*).

Statistics

The Students t-test for paired data and linear regression and correlations were applied to all the measurements. Statistical significance was assigned to a p level of 0.05.

RESULTS

Contrast Angiography

The biplane ventriculograms were of good quality in all 25 cases. The contrast angiographic LV volumes ranged between 31 ml at ES and 357 ml at ED. The EFs obtained from those volumes varied from 0.33 to 0.75. Wall motion analysis revealed 11 normokinetic ventricles, 1 diffusely hypokinetic ventricle, 8 segmentally hypokinetic or akinetic ventricles, and 5 cases with segmental dyskinesia.

The final angiographic diagnoses were coronary artery disease in 22, dilated cardiomyopathy in 1, and no cardiac disease in 2 cases.

Radionuclide Angiography

The radionuclide angiography was of good quality in 24 of the 25 cases. One patient had poor statistics in the left ventricle because maximal activity was recorded in the pulmonary outflow tract.

Ejection Fraction. The comparison between the biplane ventriculographic EFs and the radionuclide EFs using the standard manual ROI method (Table 1) showed a correlation coefficient (r) of 0.88 and a s.e.e. of 0.08 [EF (RNA) = 1.1 EF (contrast) − 0.09]. A paired analysis showed no significant difference (p = 0.16). The discrepancies were all <0.15 except in one case where the RNA LVEF underestimated the contrast LVEF by 0.20 in a patient with severe apical dyskinesia. The automated ROI method for calculating the radionuclide EF was also correlated with the contrast EF. The r was 0.86, the s.e.e. was 0.08 [EF (RNA) = 0.98 EF (contrast) − 0.02], and in this case there was a significant difference between the two (p = 0.013).

Volumes. In this method, Equation 5 (see Count Proportional Volume Theory) was applied to the manually-drawn ED and ES LV ROI. The correlation between the 50 contrast angiographic LV volumes (all ED plus ES volumes) and the RNA volumes showed an r of 0.95, a s.e.e. of 23 ml [Volume (RNA) = 0.94 Volume (contrast) + 1.3] and a p value of 0.045 (Fig. 1A). The correlation obtained after excluding the case with poor statistics in the LV at ES was similar but the p value was 0.06. Comparing the ED volumes alone gave a correlation coefficient of 0.93, a s.e.e. of 24 ml and a slope of 0.94. There was a significant difference (p = 0.01) between the two measurements.

The correlation between ES volumes gave an r of 0.93, a s.e.e. of 23 ml and a slope of 1.1. In this case, the volumes were not significantly different (p = 0.46).

This method was also applied to the automatically drawn left ventricular ROI (Fig. 1B). Here, the volumes showed a similar correlation coefficient to that obtained with the manually-drawn ROI (0.93) and a similar s.e.e., but the slope of the regression equation was much lower and the difference much more significant (p = 0.0002). The biplane contrast volumes (all ED and ES volumes) averaged 124 ± 73 ml while the nuclear volume from automatic ROIs averaged 97 ± 58 ml, (Table 2).

For all the volume calculations, the counts from the respective ED and ES frames were applied to Equation

TABLE 1
Correlations Between Radionuclide and Contrast Angiographic Ejection Fractions

	RNA (manual ROI)	CATH	RNA (automated ROI)
mean LVEF	0.54	0.56	0.52
±s.d.	0.17	0.13	0.15
n		25	25
r		0.88	0.86
B		1.10	0.98
A		−0.09	−0.02
s.e.e.		0.08	0.08
p		0.16	0.01

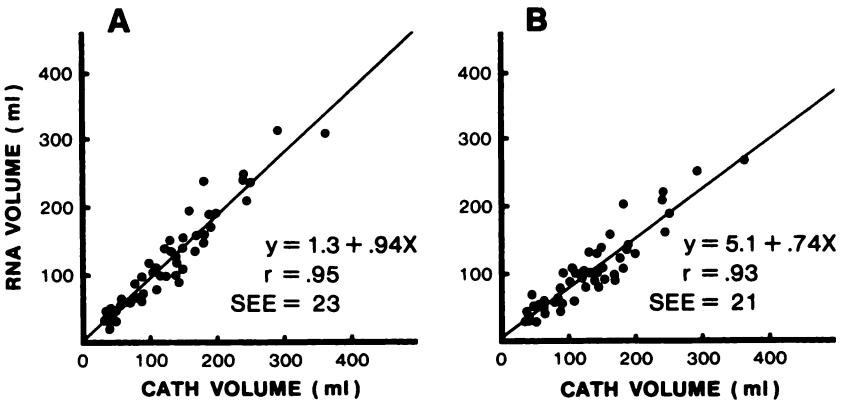

FIGURE 1
Linear regression analyses between all (end-diastolic plus end-systolic) contrast angiographic (cath) volumes and radionuclide (RNA) volumes using either manual (A) or automated (B) ROI.

5 without background correction. (Background correction was only used for EF calculations). If one compares the EFs calculated from the ED and ES volumes obtained with manual ROI, then the nuclear volumetric EF showed an r of 0.81, a s.e.e. of 0.09, and a slope of 0.96 when compared to contrast angiographic volumetric EFs (Fig. 2A). Those same volumetric nuclear EFs were also compared to the standard method of calculating nuclear EF using identical ROI. The correlation coefficient was 0.93, the s.e.e. was 0.06, and the slope 0.85 (Fig. 2B).

ES Volume Determinations from ED Volume and EF. In this case, the nuclear ED volume was calculated with a manual ROI at ED. The ES volume was then calculated by multiplying the nuclear ED volume and the standard nuclear EF to give the stroke volume and then subtracting that stroke volume from the nuclear ED volume (Fig. 3). The correlation between those results and the contrast ES volume showed a better correlation coefficient (0.95) and a smaller s.e.e. (20 ml) with the same slope (1.1) than was obtained when the nuclear ES volume was calculated directly from an ES ROI.

Observer Variability. For the volume calculations using the manually-drawn ROI, the intraobserver variability showed an r of 0.99, and a s.e.e. of 11 ml, (Fig. 4A). There was no significant difference between the two measurements. Interobserver variation showed a s.e.e. of 12 ml while the correlation coefficient was the same as for the intraobserver comparison (Fig. 4B).

TABLE 2
Left Ventricular Volumes Compared to Contrast Angiographic Volumes

	RNA (manual ROI)	CATH	RNA (automated ROI)
ED + ES Volumes	120 ± 73*	124 ± 73	97 ± 58**
ED Volume	160 ± 65*	170 ± 65	130 ± 52**
ES Volume	81 ± 60	80 ± 52	68 ± 49**

*$p \leq 0.05$.
**$p < 0.001$ compared to cath.

DISCUSSION

The measurement of left ventricular volume has always been of interest to clinicians and investigators. Almost every diagnostic modality that can provide some estimate of cardiac dimensions has been applied to the calculation of cardiac chamber volumes. The x-ray techniques, because of their excellent spatial resolution, have been regarded as most accurate and biplane contrast left ventriculography is generally used as the independent variable (gold standard) when a new technique is investigated. However, the traditional use of the prolate ellipsoid model of a LV suffers from the fact that the human LV can assume a myriad of shapes at both ED and especially at ES due to the variable manner in which disease states, most notably coronary artery disease, can alter left ventricular geometry and contraction. Furthermore, it requires left heart catheterization and, hence, is not well suited for repeated or serial evaluations.

Radionuclide approaches can be independent of geometric considerations and, thus, have great appeal. Furthermore, they are less traumatic. In vitro, count-proportional approaches to the measurement of chamber volume can be quite accurate and reproducible (*11,14,19,34*). However, in vivo, several factors can affect such methods (*19,20,27,35*). Most important are attenuation, scatter, and background activity, but the inaccuracies of ROI assignments and chamber depth measurements as well as the compromise due to studies with suboptimal statistics are additional sources of error.

The radionuclide method used in this study is based on a reference volume theory, which uses a ratio between the total counts recorded from a chamber and the counts in the hottest pixel. This approach has been previously applied to first-pass data (*30,31*), and in this report we extend its application to equilibrium acquisitions.

The formal mathematical proof of the reference volume is only valid for the idealized conditions of no scatter, attenuation, or background activity and with the volume perpendicular to the collimator face. In the

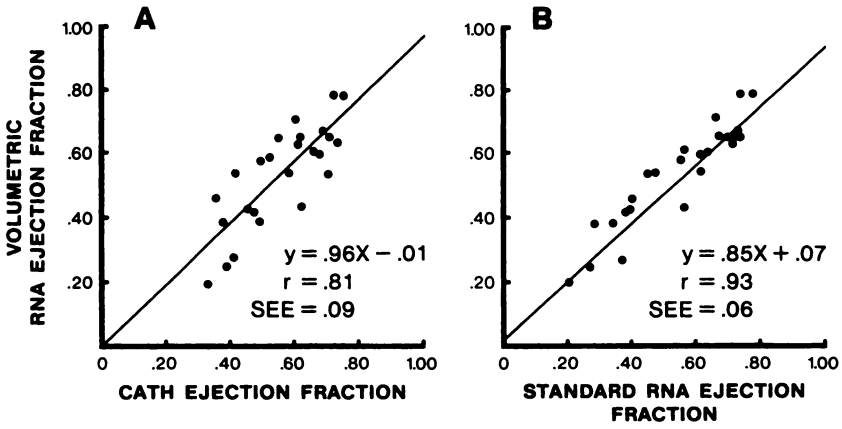

FIGURE 2
(A) LVEFs calculated from the radionuclide (RNA) determined ED and ES volumes are compared to the EFs calculated from contrast angiographic (cath) ED and ES volumes. (B) LVEFs determined from RNA ED and ES volumes are compared to LVEFs determined by the standard RNA count-based method.

gated blood-pool measurement, the left ventricle is usually sampled in the LAO position. The raw counts observed are influenced by a number of complicating factors such as scatter, self-attenuation in the ventricular chamber, attenuation from the myocardial wall, and background from the adjacent anatomy. Furthermore, the diameter of the LV in the LAO position, corresponding to maximum pixel counts, is intermediate in length between the length of the minor axis and the length of the major axis. A preliminary analysis of the complicating factors suggested that the best approach to analyzing the data from the LAO position was the simple spherical model of Equation 5 using the raw pixel data with no corrections of any kind for background, scatter, attenuation, or ventricular chamber eccentricity. Three considerations led to this simplest of approaches:

1. Extensive measurements on balloons and cylinders in different sizes and shapes, immersed in different amounts of water showed that self-attenuation and scatter within the tracer volume and distance changes between the collimator and the balloon within the physiologic range have a negligible effect on the true ratio of total counts to hottest pixel counts over a wide range of volumes.

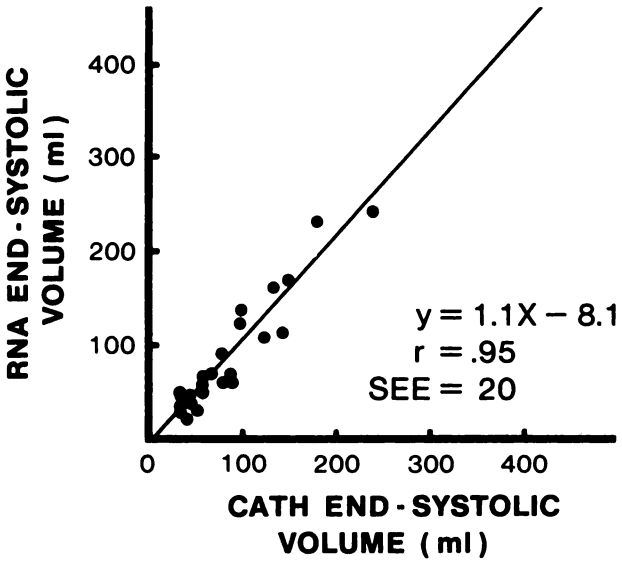

FIGURE 3
The ES volume calculated from the radionuclide (RNA) ED volume and the RNA ejection fraction is compared to the contrast angiographic (cath) ES volume.

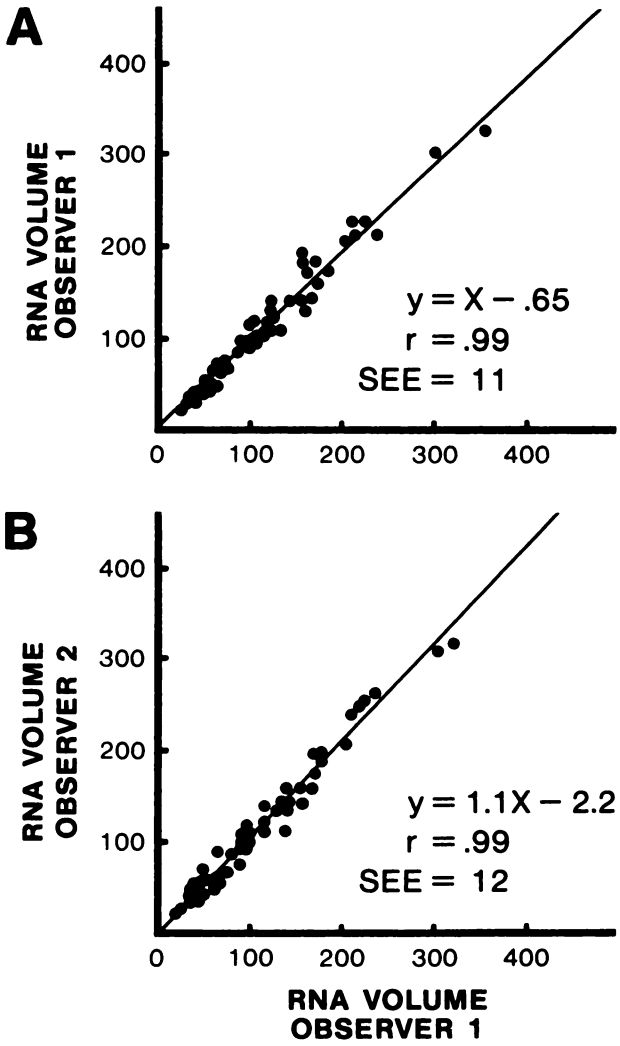

FIGURE 4
Intraobserver (A) and interobserver (B) variability for the radionuclide LV volume calculation.

2. The effect on observed counts from background and attenuation in the extraventricular chambers tend to cancel each other since background increases counts and attenuation decreases counts.
3. The intermediate value of the left ventricular axis observed in the maximum pixel from the LAO view tends to effectively approach the length of the sphere with the same volume as the ventricular chamber.

End-Diastolic Versus End-Systolic Volumes

Intuitively, one would anticipate that the ED volume measurement would be more accurate than the ES measurement because of better statistics and more reliable ROI. That was, in fact, the case. The s.e.e. for ES volume ranged from 23% to 27% of the average contrast angiographic ES volume while those for ED ranged from 10% to 18%.

Since the EF calculation using manually-drawn ROIs was not significantly different from the contrast angiographic EF, it seemed appropriate to calculate ES volume from the ED volume and the EF. The ES volumes calculated in that way were not significantly different from the contrast angiographic ES volumes ($p = 0.48$) while the s.e.e. was 25% of the mean ES volume.

Manual Versus Automatic ROIs

Both manual and automated ROI resulted in underestimation of the contrast angiographic volumes but the automated approach gave a much larger underestimate. The slopes of the linear regression equations were 0.94 for the manual method versus 0.74 for the automated method. Our automated ROI algorithm is commercially provided and based on a second-derivative edge detection approach. Improvement in that algorithm might permit a fully automated volume calculation. It is quite simple to automate the selection of the hottest pixel in the left ventricular chamber. At this time, however, manual or semiautomatic (allowing operator interaction) ROI appear preferable, especially for ES.

CONCLUSION

Several radionuclide approaches to the measurement of left ventricular volume using EqRNA have been described. To date, the published approaches require either blood sampling and counting, chamber-to-collimator distance measurement, assumptions about attenuation coefficients, or calculation of a transmission factor. Despite all the variability, the standard errors of those approaches are quite similar ranging from 10 to 36 ml, and the coefficients of the correlations with contrast angiography range from 0.80 to 0.98.

The approach described in this study has its own shortcomings but offers a reproducible method that requires no additional procedures other than the basic equilibrium acquisition itself, resulting in a s.e.e. that is comparable to previously published techniques. With improved edge detection algorithms, a fully automated approach could be developed.

REFERENCES

1. Strauss HW, Zaret BL, Hurley PW, et al. A scintigraphic method for measuring left ventricular ejection fraction in man without catheterization. *Am J Cardiol* 1971; 28:575–580.
2. Sullivan RW, Bergeron DA, Vetter WR, et al. Peripheral venous scintillation angiocardiography in determination of left ventricular volume in man. *Am J Cardiol* 1971; 28:563–567.
3. Glass FC, Joye JA, Berman DS, et al. Accuracy of noninvasively determined left ventricular volumes by gated radionuclide cineangiography in coronary, valvular and myocardial heart diseases [Abstract]. *Am J Cardiol* 1978; 41:381.
4. Ashburn WL, Kostub WJ, Karliner JS, et al. Left ventricular volume and ejection fraction determination by radionuclide angiography. *Semin Nucl Med* 1973; 3(2):165–176.
5. Seldin DW, Esser PD, Nichols AB, et al. Left ventricular volume determination from scintigraphy and digital angiography by a semi-automated geometric method. *Radiology* 1983; 49:809–813.
6. Petru MA, Sorensen SG, Chaudhuri TK, et al. Attenuation correction of equilibrium radionuclide angiography for noninvasive quantification of cardiac output and ventricular volumes. *Am Heart J* 1984; 107:1221–1228.
7. Ishii Y, MacIntyre W. Measurements of heart chamber volumes by analysis of dilution curves simultaneously recorded by scintillation camera. *Circulation* 1971; 44:37–46.
8. Steele P, Kirch D, Matthews M, et al. Measurement of left heart ejection fraction and end-diastolic volume by a computerized, scintigraphic technique using a wedged pulmonary arterial catheter. *Am J Cardiol* 1974; 34:179–186.
9. Gorten R, Stauffer J. A study of the techniques and sources of error in the clinical application of the external counting method of estimating cardiac output. *Am J Med Sci* 1959; 238:274–279.
10. Sorensen SG, Ritchie JL, Caldwell JH, et al. Serial exercise radionuclide angiography. Validation of count derived changes in cardiac output and quantitation of maximal exercise ventricular volume change after nitroglycerine and propanolol in normal men. *Circulation* 1980; 61:600–609.
11. Slutsky R, Karliner J, Ricci D, et al. Left ventricular volumes by gated equilibrium radionuclide angiography. *Circulation* 1979; 60:556–564.
12. Dehmer GJ, Lewis SE, Hillis LD, et al. Non-geometric determination of left ventricular volumes from equilibrium blood pool scans. *Am J Cardiol* 1980; 45:293–300.
13. Dehmer GJ, Firth BG, Lewis SE, et al. Direct measurement of cardiac output by gated equilibrium blood pool scintigraphy: validation of scintigraphic volume measurements by a non-geometric technique. *Am J Cardiol* 1981; 47:1061–1066.
14. Links JM, Becker LC, Shindledecker JG, et al. Measurements of absolute left ventricular volume from gated blood pool studies. *Circulation* 1982; 65:82–91.
15. Burow RD, Wilson MF, Heath CR, et al. Influence of attenuation on radionuclide stroke volume determinations. *J Nucl Med* 1982; 23:781–785.
16. Thomsen JH, Patel AK, Rowe BR, et al. Estimation of absolute left ventricular volume from gated radionuclide ventriculograms: a method using phase image assisted automated edge detection and two-dimensional echocardiography. *Chest* 1983; 84:6–12.

17. Parrish MD, Graham TP, Born ML, et al. Radionuclide ventriculography for assessment of absolute right and left ventricular volumes in children. *Circulation* 1982; 66:811–819.
18. Burns RJ, Druck MN, Woodward DS, et al. Repeatability of estimates of left ventricular volume from blood-pool counts: concise communication. *J Nucl Med* 1983; 24:775–781.
19. Verani MS, Gaeta J, LeBlanc AD, et al. Validation of left ventricular volume measurements by radionuclide angiography. *J Nucl Med* 1985; 26:1394–1401.
20. Schneider RM, Jaszczak RJ, Coleman RE, et al. Disproportionate effects of regional hypokinesis on radionuclide ejection fraction: compensation using attenuation-corrected ventricular volumes. *J Nucl Med* 1984; 25:747–754.
21. Nickoloff EL, Perman WH, Esser D, et al. Left ventricular volume: physical basis for attenuation corrections in radionuclide determinations. *Radiology* 1984; 152:511–515.
22. Keller AM, Simon TR, Smitherman TC, et al. Direct determination of the attenuation coefficient for radionuclide volume measurements. *J Nucl Med* 1987; 28:102–107.
23. Maurer AH, Siegel JA, Denenberg BS, et al. Absolute left ventricular volume from gated blood-pool imaging with use of esophageal transmission measurement. *Am J Cardiol* 1983; 51:853–858.
24. Harpen MD, Dubuisson RL, Had GB, et al. Determination of left ventricular volume from first-pass kinetics of labeled red cells. *J Nucl Med* 1983; 24:98–103.
25. Siegel JA, Wu RK, Maurer AH. The buildup factor: effect of scatter on absolute volume determination. *J Nucl Med* 1985; 26:390–394.
26. Siegel JA. The effect of source size on the buildup factor: calculation of absolute volume. *J Nucl Med* 1985; 26:1319–1322.
27. Stadius ML, Williams DL, Harp G, et al. Left ventricular volume determinations using single-photon emission computed tomography. *Am J Cardiol* 1985; 55:1185–1191.
28. Bourguignon MH, Schindledecker G, Carey GA, et al. Quantification of left ventricular volume in gated equilibrium radioventriculography. *Eur J Nucl Med* 1981; 6:349–353.
29. Nickel O, Schad N, Andrews EJ, et al. Scintigraphic measurement of left ventricular volumes from the count-density distribution. *J Nucl Med* 1982; 23:404–410.
30. Grenier R, Schmidt DH, Dymond D. Non-geometric measurement of left ventricular volume from first pass radionuclide angiography [Abstract]. *Am J Cardiol* 1982; 49:1031.
31. Gal R, Grenier R, Schmidt DH, et al. Count-based left ventricular volume measurement without blood sampling or attenuation correction from first-pass radionuclide angiography [Abstract]. *J Nucl Med* 1986; 27:912.
32. Massardo T, Gal R, Grenier R, et al. Left ventricular volume calculation from gated radionuclide angiography without blood sampling or distance measurement [Abstract]. *J Nucl Med* 1988; 29:745.
33. Dodge HT, Sandler H, Baxley WA, et al. The use of biplane angiocardiography for the measurement of the left ventricular volume in man. *Am Heart J* 1962; 60:762.
34. Fearnow EC, Stanfield JA, Jaszczak RJ, et al. Factors affecting ventricular volumes determined by a count-based equilibrium method. *J Nucl Med* 1985; 26:1042–1047.
35. Bennett G, Siegel A. The heart of count based left ventricular volume quantitation is proper attenuation correction [Abstract]. *Clin Nucl Med* 1987; 12(9S):14.